The Journal of Experimental Biology 209, 3610-3620
Published by The Company of Biologists 2006
doi:10.1242/jeb.02394

A reaction–diffusion analysis of energetics in large muscle fibers secondarily evolved for aerobic locomotor function

Kristin M. Hardy[1,*], Bruce R. Locke[2], Marilia Da Silva[2] and Stephen T. Kinsey[1]

[1]*Department of Biology and Marine Biology, University of North Carolina Wilmington, 601 South College Road, Wilmington, NC 28403-5915, USA and* [2]*Department of Chemical and Biomedical Engineering, FAMU-FSU College of Engineering, Tallahassee, FL 32310-6046, USA*

*Author for correspondence (e-mail: kmh6265@uncw.edu)

Accepted 20 June 2006

Summary

The muscles that power swimming in the blue crab, *Callinectes sapidus*, grow hypertrophically, such that in juvenile crabs the cell diameters are <60 μm, whereas fibers of the adult crabs often exceed 600 μm. Thus, as these animals grow, their muscle fibers greatly exceed the surface area to volume ratio and intracellular diffusion distance limits of most cells. Previous studies have shown that arginine phosphate (AP) recovery in the anaerobic (light) fibers, which demonstrate a fiber size dependence on anaerobic processes following contraction, is too slow to be restricted by intracellular metabolite diffusive flux, in spite of the fiber's large size. By contrast, the aerobic (dark) fibers have evolved an intricate network of intracellular subdivisions that maintain an effectively small 'metabolic diameter' throughout development. In the present study, we examined the impact of intracellular metabolite diffusive flux on the rate of post-contractile AP resynthesis in the dark muscle, which has a much higher aerobic capacity than the light muscle. AP recovery was measured for 60 min in adults and 15 min in juveniles following burst contractile activity in dark fibers, and a mathematical reaction–diffusion model was used to test whether the observed aerobic rates of AP resynthesis were fast enough to be limited by intracellular metabolite diffusion. Despite the short diffusion distances and high mitochondrial density, the AP recovery rates were relatively slow and we found no evidence of diffusion limitation. However, during simulation of steady-state contraction, which is an activity more typical of the dark fibers, there were substantial intracellular metabolite gradients, indicative of diffusion limitation. This suggests that high ATP turnover rates may lead to diffusion limitation in muscle even when diffusion distances are short, as in the subdivided dark fibers.

Key words: muscle fiber, fiber growth, diffusion, metabolic modeling, reaction–diffusion, exercise, metabolism, scaling, crustacean, blue crab, *Callinectes sapidus*, phosphagen, arginine phosphate, glycogen, mitochondria.

Introduction

The muscles that power swimming in the blue crab, *Callinectes sapidus*, grow by increasing the diameter of individual fibers (hypertrophy), rather than by increasing fiber number (hyperplasia), and during post-metamorphic development fiber diameters increase from <60 μm in juveniles to >600 μm in adults (Boyle et al., 2003). This contrasts with muscle fibers of most organisms, which generally have a size range of 10–100 μm. Presumably, fiber size is governed by the fundamental need to carry out aerobic metabolic processes, which rely on oxygen flux across cell membranes (Kim et al., 1998), and ATP diffusive flux from mitochondria to sites of ATP demand (Mainwood and Rakusan, 1982). Thus, a likely functional consequence of excessive cell size is a reduced capacity for oxidative metabolism (Boyle et al., 2003; Johnson et al., 2004; Kinsey et al., 2005).

The swimming muscles of *C. sapidus* are composed of three distinct types of fibers: light fibers that power anaerobic burst swimming, dark fibers that power aerobically fueled endurance swimming, and a small number of fibers intermediate to the light and dark fibers (Tse et al., 1983). The anaerobic light fibers rely on endogenous fuels such as arginine phosphate (AP) and glycogen during contraction, not oxygen influx, so contractile function should not be impacted by an increase in fiber size. However, aerobically driven processes, such as post-contractile recovery, may be limited in the largest light fibers because low cell surface area to volume ratios may constrain oxygen flux into the cell and intracellular diffusion distances may become excessive (Kinsey and Moerland, 2002; Boyle et al., 2003; Kinsey et al., 2005). These cellular level limitations may therefore have behavioral costs by extending the recovery time required

between successive bursts of high velocity swimming needed for predator escape.

Whereas the dark fibers reach the same large dimensions as the light fibers, their aerobic contractile function should favor small size throughout development. To accommodate the conflicting demands for hypertrophic growth and small fiber size, dark fibers have evolved small mitochondria-rich subdivisions (Tse et al., 1983) that increase in number and maintain a constant size during development, as well as promote intra-fiber perfusion to facilitate O_2 delivery to the subdivisions (Johnson et al., 2004). Thus, blue crab dark fibers are unusual in having metabolic functional units (fiber subdivisions) that retain small dimensions throughout development, whereas their contractile functional units (fibers) appear to grow hypertrophically to extreme proportions.

Anaerobic light fibers are therefore characterized by large cell size and low ATP demand, whereas dark fibers remain effectively small (*via* subdivisions) throughout development, but have the capacity for much higher rates of ATP turnover. We have previously hypothesized that anaerobic glycogenolysis is recruited following burst contractions in large anaerobic fibers to accelerate certain key phases of recovery that would otherwise be slowed by size-related limitations to the rate of aerobic ATP synthesis (Kinsey and Moerland, 2002; Boyle et al., 2003; Johnson et al., 2004; Kinsey et al., 2005). This hypothesis is supported by observations that the rate of post-contractile AP resynthesis, which is potentially increased by anaerobic metabolism, is size-independent in blue crab anaerobic fibers (Kinsey et al., 2005). Further, significant post-contractile glycogen depletion (Boyle et al., 2003) and increased post-contractile lactate accumulation (Johnson et al., 2004), both anticipated consequences of anaerobic glycogenolysis, were found in the anaerobic fibers from adult animals, but not juveniles. It is unlikely, however, that this strategy is implemented in the large dark fibers because intracellular subdivisions maintain the small effective diameter necessary to permit aerobic metabolism during recovery. Thus, it is reasonable to expect that differences in the rate of post-contractile AP recovery in dark fibers from adult and juvenile crabs are not related to fiber size, but result from 'normal' metabolic scaling with body mass (Schmidt-Neilson, 1984). Furthermore, if anaerobic glycogenolysis is not being exploited in the large aerobic fibers, post-contractile glycogen depletion and lactate accumulation should be minimal and size independent.

Johnson et al. (Johnson et al., 2004), however, reported significant post-contractile lactate accumulation in the highly subdivided dark fibers of adult crabs (although the levels were significantly lower than seen in light fibers). The authors reasoned that this was a likely consequence of close proximity of the dark muscle to the much larger mass of lactate-producing light fibers, as well as net diffusive flux into the dark fibers from the lactate-laden hemolymph, but not the result of post-contractile anaerobic glycogenolysis occurring within the dark fibers. The absence of size-dependent glycogen depletion in dark fibers would be consistent with the conclusions of Johnson et al. (Johnson et al., 2004).

These previous observations provide strong evidence for fiber size effects in blue crab light muscle fibers, which are probably mediated through excessive intracellular diffusive distances and/or low cell surface area to volume ratios. The dark fibers have the aforementioned structural modifications that appear to offset the constraints of large fiber size, but these fibers also have high rates of ATP turnover that make them more susceptible to diffusion limitation. The present study examined the fiber size dependence of post-contractile recovery in the dark muscle fibers of juvenile and adult blue crabs. The objectives were to (1) measure the rate of AP recovery, (2) apply a mathematical reaction–diffusion model to determine whether the rate of AP recovery is limited by intracellular metabolite diffusive flux, and (3) measure post-contractile glycogen depletion. We hypothesized that (1) differences in the rate of post-contractile AP recovery in dark fibers are principally the result of differences in mass-specific aerobic capacity due to metabolic scaling (Schmidt-Neilson, 1984); (2) intracellular metabolite diffusive flux does not limit the rate of AP recovery; and (3) there is no size-dependent post-contractile depletion of glycogen in dark aerobic fibers because anaerobic metabolism is not recruited during recovery in the large fibers of the adults.

Materials and methods

Animals

Juvenile blue crabs (*Callinectes sapidus* Rathbun) were collected by sweep netting in the basin of the Cape Fear River Estuary, NC, USA. Adult crabs were obtained from baited crab traps set in Masonboro Sound, NC, USA or purchased from local fisherman (Wilmington, NC, USA). Crabs were maintained in full-strength filtered seawater (35‰ salinity, 21°C) in aerated, recirculating aquariums. They were fed bait shrimp three times weekly and kept on a 12 h:12 h light:dark cycle. All animals were held under these conditions for at least 72 h before experimentation. Animals were sexed, and their carapace width and body mass were measured prior to use (Table 1). Only animals in the intermolt stage were used as determined by the rigidity of the carapace, the presence of the membranous layer of the carapace, and the absence of a soft cuticle layer developing beneath the existing exoskeleton (Roer and Dillaman, 1984).

Exercise protocol

Crabs were induced to undergo a burst swimming response as described previously (Boyle et al., 2003; Johnson et al., 2004; Kinsey et al., 2005). Crabs were held suspended in the air by a clamp in a manner that allowed free motion of the swimming legs and small wire electrodes were placed in two small holes drilled into the mesobranchial region of the dorsal carapace. A Grass Instruments SD9 physiological stimulator (Astro Med, Inc., West Warwick, RI, USA) was used to deliver a small voltage (80 Hz, 200 ms duration, 10 V cm^{-1} between

Table 1. *Size classes of crabs*

	Arginine phosphate use and recovery				Glycogen use and recovery			
Size class	*N*	Carapace width (mm)	Body mass (g)	Body mass range (g)	*N*	Carapace width (mm)	Body mass (g)	Body mass range (g)
Small	41	28.3±0.5	2.0±0.1	1.0–3.6	60	29.0±0.4	2.2±0.1	1.1–3.6
Large	36	139.2±1.9	187.0±6.7	89.0–254.1	60	142.7±1.3	182.2±4.6	136.2–284.5

electrodes) to the thoracic ring ganglia, which elicited a burst swimming response in the fifth periopods for several seconds following the stimulation. A single pulse was administered every 20–30 s until the animal was no longer capable of a burst response, which was evident when it responded by moving its legs at a notably slower rate. During exercise, animals were exposed to the air for a period of only 3–4 min, which is sufficiently short to avoid compromised gill oxygen transport due to changing scaphognathite activity, lamellar clumping or lactate accumulation (deFur et al., 1988). Immediately following exercise, animals were returned to aerated full-strength seawater and allowed to recover. Animals assayed for AP were sampled at 0, 15, 30 or 60 min (adults) and 0, 5, 10 or 15 min (juveniles) post-contraction, whereas animals assayed for glycogen were sampled at 0, 30, 60, 120 or 240 min post-contraction.

Metabolite measurement

At the end of the recovery period, crabs were rapidly cut in half along their sagittal plane in order to minimize the spontaneous burst contraction of the swimming legs that typically occurs as they are killed. The dorsal carapace, reproductive and digestive organs were removed and the basal cavity that houses the muscles of the fifth periopod was exposed. The dark levator muscle was rapidly isolated by cutting away the surrounding muscle and freeze-clamped using tongs cooled in liquid nitrogen while still intact within the animal. The time elapsed from death to freeze clamping the muscle was 60–90 s. After tissue extraction, samples being analyzed for glycogen were stored at –80°C until further evaluation. Samples assayed for AP were immediately homogenized in a 6- to 35-fold dilution of chilled 7% perchloric acid with 1 mmol l^{-1} EDTA using a Fisher Powergen 125 homogenizer, and then centrifuged at 16 000 ***g*** for 30 min at 4°C. The supernatant pH was neutralized with 3 mol l^{-1} potassium bicarbonate in 50 mmol l^{-1} Pipes, stored on ice for 10 min, and centrifuged at 16 000 ***g*** for 15 min at 4°C. The supernatant was immediately analyzed by ^{31}P nuclear magnetic resonance (NMR) spectroscopy. NMR spectra were collected at 162 MHz on a Bruker 400 DMX spectrometer (Bruker Instruments, Billerica, MA, USA) to determine relative concentrations of AP, inorganic phosphate (P_i), and ATP. Spectra were collected using a 90° excitation pulse and a relaxation delay of 12 s, which ensures that the phosphorus nuclei were fully relaxed and peak integrals for the metabolites were proportional to their relative concentrations. Forty-eight scans were acquired for a total acquisition time of 10 min. The area under each peak was integrated using Xwin-NMR software to yield relative concentrations of each metabolite.

Previously frozen tissue samples were analyzed for glycogen based on the method of Keppler and Decker (Keppler and Decker, 1974). Samples were homogenized in a 5- to 31-fold dilution of 3.6% perchloric acid then divided into two pools: a blank aliquot for measuring free glucose, and a sample aliquot for measuring total glucose content (free glucose+glycogen). The total glucose sample aliquot was neutralized with 1 mol l^{-1} potassium bicarbonate and incubated at 40°C for 2 h in an amyloglucosidase solution (14 units ml^{-1} in 0.2 mol l^{-1} acetate buffer, pH 4.8) while undergoing constant shaking. After incubation was complete, the reaction was stopped by the addition of 3.6% perchloric acid and both the glucose blank and the total glucose sample were centrifuged at 16 000 ***g*** for 15 min. Before being assayed supernatants from both pools were neutralized with 1 mol l^{-1} $KHCO_3$. Both aliquots were then added to a solution containing 1 mol l^{-1} ATP, 0.9 mmol l^{-1} β-NADP, 15.6 units glucose 6-phosphate dehydrogenase, 0.3 mol l^{-1} triethanolamine hydrochloride, and 4.05 mmol l^{-1} $MgSO_4$ at pH 7.5. The reaction was started by the addition of 15.8 units of hexokinase. The amount of glucose in each pool is proportional to the increase in NADPH, which was measured spectrophotometrically at a wavelength of 340 nm. Subtraction of the free glucose in the blank from glucose hydrolyzed from glycogen in the total glucose sample aliquot yielded glycogen content in units of μmol glucosyl g^{-1} of tissue.

Mathematical modeling

The reaction–diffusion model used in the present study was as described in Kinsey et al. (Kinsey et al., 2005), with parameters adjusted to comply with blue crab dark levator fibers. In brief, the model calculated the diffusion and reaction of ATP, ADP, AP, arginine (Arg) and P_i in a one-dimensional system that extended from the surface of a mitochondrion to a distance (λ/2) equal to half of the mean free spacing between clusters of mitochondria, which were assumed to be distributed at the periphery of each subdivision (Fig. 1). Four kinetic expressions were used to determine reaction rates, and these expressions were either boundary reactions (i.e. the production of ATP at the mitochondrial membrane), or bulk reactions (those reactions that occur throughout the cytoplasm). Michaelis-Menten expressions were used for the mitochondrial boundary reaction ($ADP+P_i \rightarrow ATP$) with a rate dependent on the ADP concentration, a myosin ATPase bulk reaction ($ATP \rightarrow ADP+P_i$) that is only active during contraction, and a basal ATPase bulk reaction that is always active. In addition,

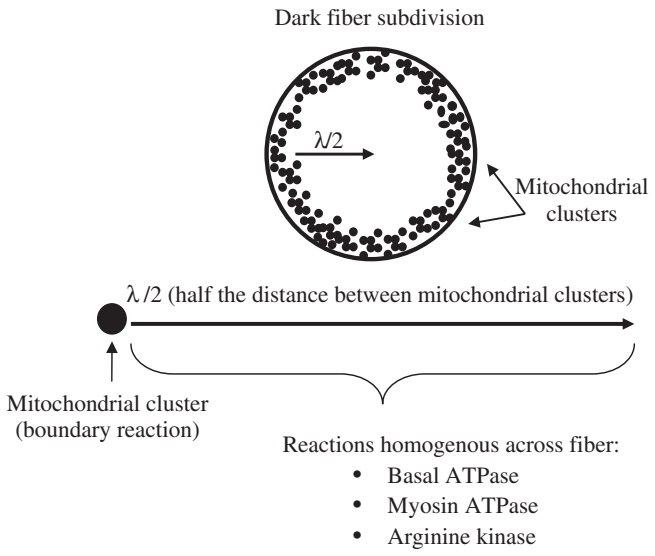

Fig. 1. Schematic of the reaction–diffusion mathematical model. Metabolite concentrations during a contraction–recovery cycle in dark levator fibers were modeled over the length λ/2, which represents half of the distance between mitochondrial clusters.

a complete kinetic expression for arginine kinase (AK) was included in the bulk phase (Smith and Morrison, 1969). Diffusion coefficients for radial motion (perpendicular to the fiber long axis; $D_{\perp}$) incorporated the time-dependence of diffusion found in skeletal muscle (Kinsey et al., 1999; Kinsey and Moerland, 2002). Temporally and spatially dependent concentration profiles of metabolites were calculated using molar-species continuity equations for all five metabolites (Bird et al., 1960).

Simulations of a burst contraction–recovery cycle were generated using the finite element analysis software, FEMLAB (Comsol, Inc., Burlington, MA, USA). The myosin ATPase was activated at 10 Hz for several seconds, while the basal ATPase was active throughout the entire contraction-recovery cycle. Model input parameters are detailed in Table 2. The resting metabolite concentrations for crustacean aerobic locomotor fibers were obtained from data gathered during this study and calculations using the AK equilibrium constant (Teague and Dobson, 1999). Metabolite data, expressed as μmol g^{-1} muscle tissue, were converted to mmol l^{-1} by assuming that intracellular water accounted for 68% of the wet mass in blue crab dark levator muscle (Milligan et al., 1989). Resting arginine concentrations were set at a reasonable, but arbitrary value (Beis and Newsholme, 1975). The $D_{\perp}$ values for each metabolite were based both on direct measurements from crustacean anaerobic fibers and calculations from the relationship of molecular mass and $D_{\perp}$ in these fibers (Kinsey and Moerland, 2002). Intracellular diffusion distances were estimated according to Johnson et al. (Johnson et al., 2004), who found a mean subdivision diameter of 35.6 μm and a primarily subsarcolemmal distribution of mitochondria in the subdivisions of both small and large fibers in the dark muscle. A K_m for the mitochondrial reaction ($K_{m,mito}$) for ADP of 50 μmol l^{-1} was used, which is within the range for slow-twitch skeletal muscle (Kushmerick et al., 1992). The basal ATPase maximal velocity ($V_{m,bas}$) and K_m ($K_{m,bas}$) for ATP were estimated so as to maintain constant resting concentrations over time in an inactive fiber and to promote a return to the initial steady state following contraction, and these values are similar to basal ATPase rates estimated for skeletal muscle (Vicini and Kushmerick, 2000). AK dissociation constants were obtained from Smith and Morrison (Smith and Morrison, 1969), the maximal velocity for the reverse reaction ($V_{m,AK,rev}$) was taken from measurements in blue crab dark levator muscle (Holt and Kinsey, 2002), and the maximal velocity for the forward reaction ($V_{m,AK,for}$) was calculated from the AK Haldane relationship from Smith and Morrison (Smith and Morrison, 1969) using an equilibrium constant for AK of 40 (Teague and Dobson, 1999). The myosin ATPase maximal velocity ($V_{m,myo}$) and K_m ($K_{m,myo}$) for ATP were the same as used for aerobic muscle by Hubley et al. (Hubley et al., 1997).

Although the model generated temporally and spatially resolved concentrations of metabolites, our experimental measurements yielded values that were spatially averaged across the fiber. In order to compare the model results with the experimental data, some of the model data was mathematically volume averaged to remove the spatial dependence in concentration while retaining the temporal variation. (Note that since the model is one-dimensional, this averaging process required integration only over that one dimension.) For model simulations that were volume averaged, the duration of myosin ATPase activation was adjusted so that the decrease in AP concentration ([AP]) was comparable to that in the observed data and the values for the maximal velocity of the mitochondrial reaction ($V_{m,mito}$) values were adjusted so that the AP recovery curve, predicted by the model, approximated the measured recovery rate. This approach facilitated the analysis of diffusion limitation of the rate of AP recovery. Since the dark levator muscle is active during sustained aerobic swimming, steady-state contractions, in which myosin was continuously active, were also simulated, and $V_{m,mito}$ and $V_{m,myo}$ were adjusted to model different rates of ATP turnover. These latter simulations were arbitrarily modeled in the small fibers, because of the similarity in the model parameters between the large and small fibers and because the higher rate of oxidative phosphorylation in the small fibers make them more likely to be influenced by intracellular metabolite diffusion.

Analysis

Measurements of AP during recovery were not collected at the same time points for both small and large animals, so a *t*-test was used to compare the fractional recovery at 15 min post-exercise, a recovery time point that was shared between size classes. For other metabolite data, a one-way ANOVA was used to test for the main effects of recovery time. Where significant differences were detected, Tukey's HSD tests were used to compare post-contractile recovery time points to the resting value. All metabolite data are presented as means ± s.e.m. with a significance accepted at $P<0.05$.

Table 2. *Parameters used in reaction–diffusion model*

Parameter type	Parameter	Small fiber	Large fiber	Units
Initial concentrations	AP	26.9	43.97	mmol l^{-1}
	Arginine	0.5	0.5	mmol l^{-1}
	P_i	21.37	19.56	mmol l^{-1}
	ATP	10.79	11.13	mmol l^{-1}
	ADP	0.0045	0.00285	mmol l^{-1}
Diffusion	$D_{\perp AP}$	1×10^{-6}	1×10^{-6}	cm^2 s^{-1}
	$D_{\perp Arg}$	1.27×10^{-6}	1.27×10^{-6}	cm^2 s^{-1}
	$D_{\perp P_i}$	1.62×10^{-6}	1.62×10^{-6}	cm^2 s^{-1}
	$D_{\perp ATP}$	0.7×10^{-6}	0.7×10^{-6}	cm^2 s^{-1}
	$D_{\perp ADP}$	0.79×10^{-6}	0.79×10^{-6}	cm^2 s^{-1}
	$\lambda/2$	17	17	μm
Mitochondrial boundary reaction	$V_{m,mito}$	6×10^{-17}	1.97×10^{-17}	mmol μm^{-2} s^{-1}
	$K_{m,mito}$	50	50	μmol l^{-1}
Basal ATPase	$V_{m,bas}$	7	7	μmol l^{-1} s^{-1}
	$K_{m,bas}$	10	10	mmol l^{-1}
Arginine kinase reaction	$V_{m,AK,for}$	373	373	mmol l^{-1} s^{-1}
	$V_{m,AK,rev}$	23.5	23.5	mmol l^{-1} s^{-1}
	K_{ATP}	0.32	0.32	mmol l^{-1}
	K_{Arg}	0.75	0.75	mmol l^{-1}
	K_{AP}	3.82	3.82	mmol l^{-1}
	K_{ADP}	0.40	0.40	mmol l^{-1}
	K_{iATP}	0.34	0.34	mmol l^{-1}
	K_{iArg}	0.81	0.81	mmol l^{-1}
	K_{iAP}	0.26	0.26	mmol l^{-1}
	K_{iADP}	0.024	0.024	mmol l^{-1}
	K_{IATP}	2.43	2.43	mmol l^{-1}
	K_{IArg}	3.45	3.45	mmol l^{-1}
	K_{IAP}	1.46	1.46	mmol l^{-1}
Myosin ATPase	$V_{m,myo}$	3.81	3.81	mmol l^{-1} s^{-1}
	$K_{m,myo}$	0.15	0.15	mmol l^{-1}

See text for additional details and source information.

Results

Metabolite recovery

Size classes were defined based on the relationship between animal mass and light levator fiber size determined by Boyle et al. (Boyle et al., 2003) (Table 1), where the mean fiber size in the small and large animals was approximately 150 μm and 600 μm, respectively. In these experiments, as in previous studies (Boyle et al., 2003; Johnson et al., 2004; Kinsey et al., 2005), the crab stimulation procedure elicited a burst escape response that was qualitatively similar for both size classes. The frequency of leg beats during burst swimming was higher in the juveniles, but the duration of the movement was greater in the adults, and both size classes required approximately the same number of stimulations to reach fatigue. Additionally, glycogen depletion (Boyle et al., 2003), lactate accumulation (Johnson et al., 2004) and AP depletion (Kinsey et al., 2005) (see below) during exercise were identical in muscle fibers from juvenile and adult crabs, indicating a uniform metabolic response to stimulated exercise.

During a burst exercise–recovery cycle there is a reciprocal change in AP and P_i that results from the stoichiometric coupling of cellular ATPases and the AK reaction. Contraction results in a rapid depletion of AP, and corresponding increase in P_i, which is followed by a slow recovery to pre-contractile levels. This pattern is demonstrated in examples of the ^{31}P-NMR spectra collected from perchloric acid extracts of dark muscle (Fig. 2). Table 3 shows the absolute concentrations of metabolites collected at rest, and the time course of relative changes in the AP and P_i content during a contraction–recovery cycle are shown in Fig. 3. In the large fibers, total recovery takes about 60 min, while the small fibers completely recover in about 15 min. A comparison of the percentage AP recovery at 15 min post-exercise revealed a significant difference (*t*-test, $P<0.05$) between size classes (mean values for small and large fibers were 100.94±10.14% and 46.27±8.9% of the resting value after 15 min of recovery, respectively). During the course of a contraction–recovery cycle, ATP content and the sum of AP, Pi, and ATP remained constant in both large and small fibers, as expected (Fig. 3).

The absolute amount of glycogen at rest can be found

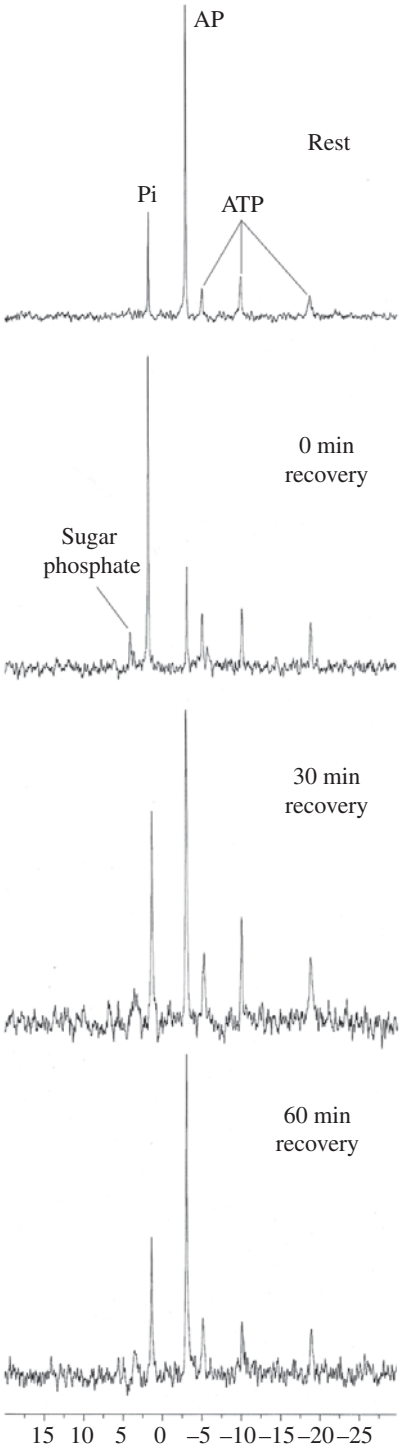

Fig. 2. Representative ^{31}P-NMR spectra collected from perchloric acid extracts of large dark levator muscle fibers that demonstrate the changes in relative concentrations of AP and P_i during a contraction–recovery cycle. Spectra were collected from crabs at rest, and after 0, 30 and 60 min of recovery from burst exercise. The same pattern of recovery was observed in the small dark fibers, except that complete AP resynthesis occurred in only 15 min. Chemical shifts are in units of parts per million.

Table 3. *Absolute resting values of AP, P_i, ATP and glycogen in small and large dark levator fibers*

	Resting values	
Metabolite	Small fiber content (μmol g^{-1})	Large fiber content (μmol g^{-1})
AP	18.3±2.3	29.9±3.1
P_i	16.5±1.8	13.3±1.4
ATP	7.2±0.8	7.3±1.1
Glycogen	33.1±4.0	69.9±9.4

in Table 3. The relative glycogen values during a contraction–recovery cycle in both size classes are illustrated in Fig. 4. The values at each time point have been normalized to the mean resting values to allow a direct comparison of post-contractile glycogen changes in small and large animals. In the large size class there was no significant depletion for up to 4 h after contraction, although there was a transient, non-significant, decrease in glycogen immediately after exercise (F=0.7611, d.f.=5, P=0.5818). In the small size class, however, there was a significant depletion of glycogen during recovery (F=6.38, d.f.=5, P=0.0001). Glycogen values at 60, 120 and 240 min after exercise were significantly lower than values in animals at rest or immediately post-exercise.

Reaction-diffusion analysis of contraction and recovery

The modeled rate of mitochondrial ATP production was adjusted to approximate our measured AP recovery curve, thereby allowing us to test whether the aerobic synthesis of AP was limited by metabolite diffusion in the dark levator fibers. The model results were volume-averaged to allow a direct comparison of the observed and simulated recovery rates. Fig. 5 shows that the model and measured data for both size classes are in close agreement, thus permitting us to draw conclusions about diffusion limitation in the aerobic fibers. The spatially and temporally resolved concentrations of high-energy phosphate molecules during a contraction–recovery cycle are also presented in Fig. 5. As expected, neither fiber exhibited intracellular concentration gradients, indicating that diffusive flux is fast relative to the rate of ATP turnover.

Although the contraction–recovery protocol used here is experimentally tractable, the primary function of the dark fibers is to power sustained, steady-state contraction. However, this is a condition we cannot replicate experimentally, so we used the model to simulate steady-state contraction. Fig. 6 shows the effect of increments in the rate of the mitochondrial boundary reaction and the myosin ATPase (i.e. turnover) on [AP] and [ATP] during steady-state contraction. The initial simulation (Fig. 6A,B), in which AP is depleted by roughly 50% during contraction, is a realistic depiction of a steady-state contraction in skeletal muscle (Meyer, 1988) and both the boundary reaction and myosin ATPase values used in this simulation are reasonable estimates (Vicini and Kushmerick, 2000). There are obvious AP gradients across the cell, indicating that at the high rate of ATP turnover characteristic of steady-state contraction, diffusion is limiting. As the mitochondrial boundary reaction

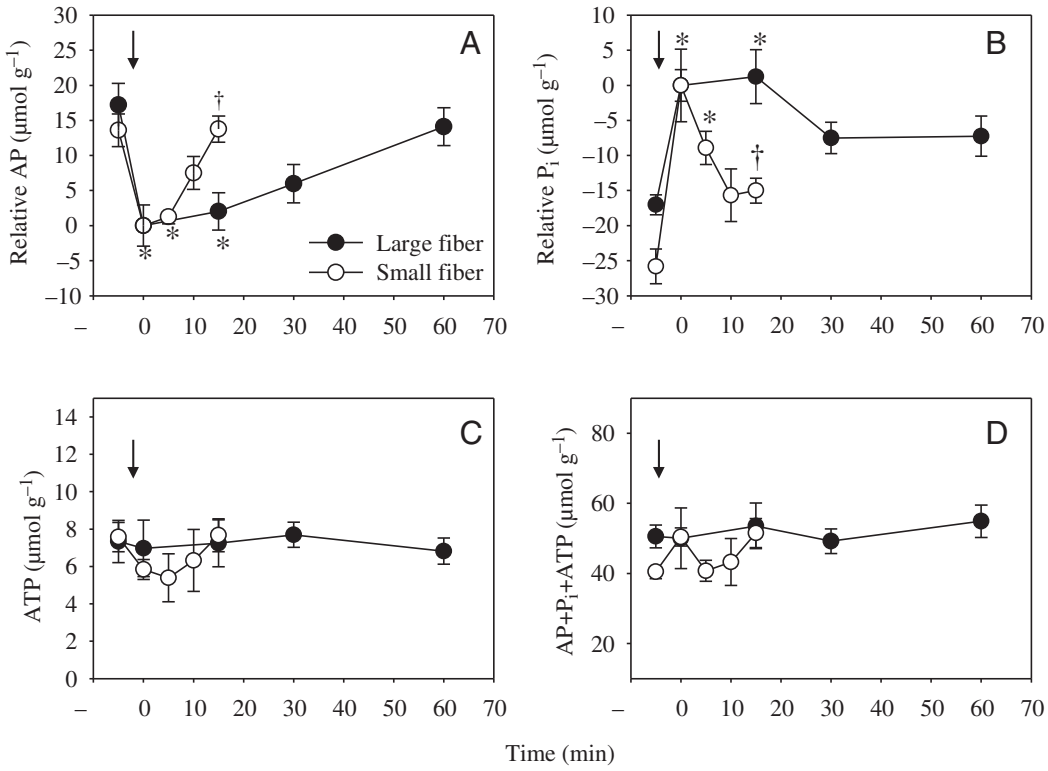

Fig. 3. Relative changes in AP (A) and P_i (B) content and absolute changes in ATP (C) and AP+P_i+ATP (D) content in small (open symbols) and large (filled symbols) dark levator fibers during a contraction–recovery cycle. In A and B, values at each time point have been normalized to the mean immediately after contraction to allow direct comparison of the recovery rate between the size classes (absolute resting values are in Table 3). Note how quickly AP and P_i levels are restored in the small fibers compared to the large fibers during recovery, as well as the relative stability in ATP and total high-energy phosphate content during contraction and recovery in both size classes. The arrow indicates when burst contractile exercise was stimulated; the asterisk indicates that values are significantly different from the resting value; and the dagger indicates that AP levels in each size class were significantly different from each other at the common 15 min recovery time point. $N \geqslant 7$ for every point.

and myosin ATPase activity are increased to simulate higher-intensity swimming, a much greater AP depletion is observed, which reduces the cell's ability to buffer [ATP], leading to substantial intracellular ATP gradients (Fig. 6C–F). Although aerobic dark fibers may not be limited by diffusive flux during recovery from burst contraction, it appears that they are limited during sustained steady-state exercise.

Discussion

The principal findings of the present study were that (1) the rate of AP recovery following exercise in the aerobic dark fibers was dependent on body mass, with differences somewhat greater than that expected from normal metabolic scaling; (2) intracellular diffusive flux does not appear to limit aerobic AP recovery after burst contraction, but it does appear to limit aerobic flux during steady-state contraction; and (3) there was no significant glycogen depletion during post-contractile recovery in the large fibers, which is consistent with our hypothesis that intracellular subdivisions alleviate the need for anaerobic contributions during recovery.

Post-contractile AP resynthesis in anaerobic light fibers from both juvenile and adult blue crabs has been shown to

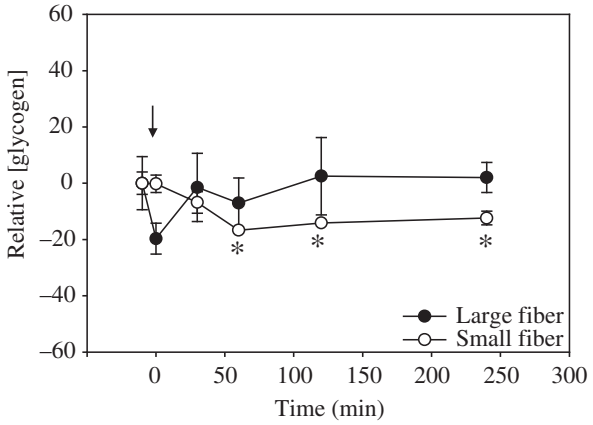

Fig. 4. Relative changes in glycogen content in small (open symbols) and large (filled symbols) dark levator fibers during a contraction–recovery cycle. Values at each time point have been normalized to the mean resting value to allow direct comparison between the size classes (absolute resting values are in Table 3). The arrow indicates when burst contractile exercise was stimulated. The asterisk indicates values significantly different from the resting value. $N \geqslant 10$ for every point.

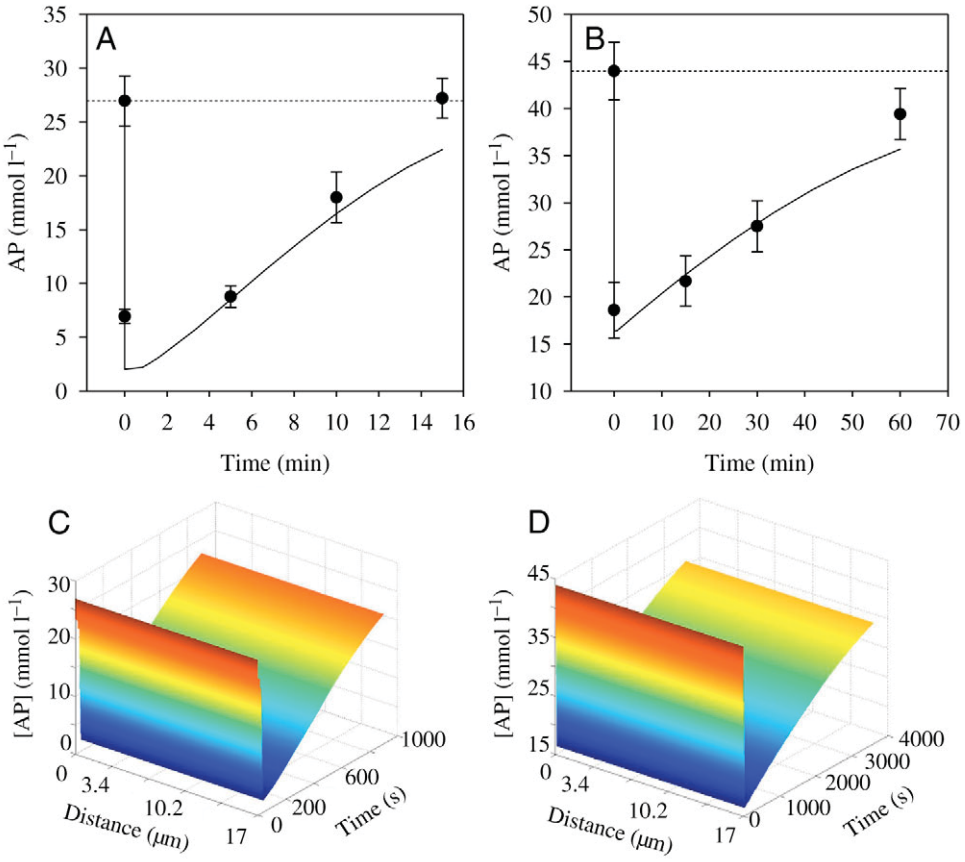

Fig. 5. Measured AP recovery (symbols) compared to the volume averaged model of AP recovery (solid line) in small (A) and large (B) dark fibers. The dotted line indicates the resting concentration. In the model, the myosin ATPase was activated long enough to cause a decrease in AP that was comparable to the measured data. (C,D) Three-dimensional graphs show the temporally and spatially resolved concentrations of AP for small (C) and large (D) dark levator fibers during a contraction–recovery cycle. This model output was generated using parameters in Table 2. Note the absence of concentration gradients.

occur in about 60 min, despite large differences in body mass and fiber size (Kinsey et al., 2005). This size independence appears to result from anaerobic contributions to recovery in large fibers (Johnson et al., 2004). Post-contractile AP resynthesis in the aerobic fibers, however, should be much faster owing to a nearly tenfold greater mitochondrial content and a twofold greater citrate synthase (CS) activity than light fibers (Boyle et al., 2003; Johnson et al., 2004). This is supported by our observation that AP recovery in the small dark fibers was complete 15 min after exercise, a rate of recovery roughly four times faster than found in the light fibers. However, the dark fibers of adults recovered at the same rate as previously observed for the light fibers. Further, the relatively fast AP recovery rate in the small dark fibers was still several fold lower than typical recovery rates in mammalian skeletal muscle with a similar mitochondrial content (e.g. Meyer, 1988; Vicini and Kushmerick, 2000; Hancock et al., 2005). Thus, the AP recovery rate appears to be influenced by both size-dependent and size-independent factors.

In the large dark fibers, intracellular subdivisions serve to create metabolic functional units with the same small diameter as the juvenile fibers, thereby permitting sustained aerobic contraction. Additionally, mitochondria represent the same total fractional volume (23–25%) in both small and large dark fiber subdivisions (Johnson et al., 2004). Thus, we expected to see a rapid AP recovery in the dark fibers from both size classes, with differences between size classes attributable to body mass-specific metabolic scaling. The mass-specific scaling exponent (*b*) for CS activity in blue crab aerobic fibers is relatively small (*b*=–0.19) (Johnson et al., 2004), whereas in many mammalian systems measurements of basal rates of O_2 consumption typically yield *b* values near –0.25 (Brody, 1945), although *b* may be as high as –0.33 (White and Seymour, 2003). Using this range of scaling exponents we calculated that small dark fibers should recover two to four times faster than large dark fibers due to scaling alone. In the present study, AP recovery in the adults took around 60 min, which is roughly four times longer than in juveniles. Whereas the observed size-dependence of AP recovery lies at the upper range of that expected from mass-specific metabolic scaling, the low scaling exponents for CS activity and mitochondrial density in blue crab fibers suggests that scaling does not fully account for the difference in the rate of AP recovery between juvenile and adult crabs.

What then can account for residual differences between size classes, and why do the aerobic fibers recover more slowly than expected? The resynthesis of phosphagens following contraction is a proton producing process. It has been shown in vertebrate systems that changes in intracellular pH (pH_i) are responsible for altering the creatine kinase equilibrium constant and hence, the phosphocreatine recovery rate (Sahlin et al., 1975; Harris et al., 1976; Meyer et al., 1986; van den Thillart and Waarde, 1993; McMahon and Jenkins, 2002). Similarly,

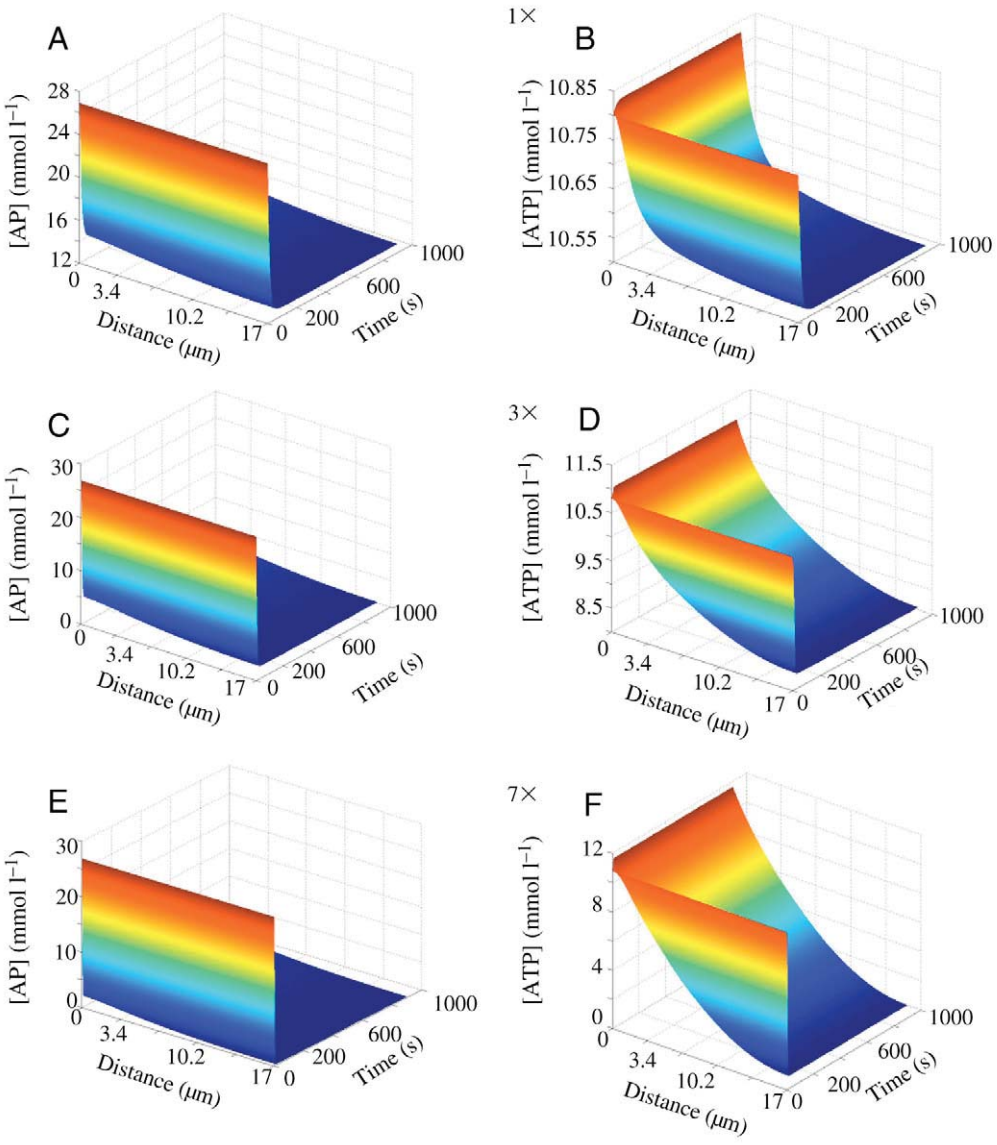

Fig. 6. The effect of increasing the rate of mitochondrial ATP production and myosin ATPase activity during steady-state contraction in small fibers on the temporal and spatial profiles of AP (A,C,E) and ATP (B,D,F). Metabolite concentrations during a typical steady-state contraction, where $V_{m,mito}$=1.00×10^{-14} mmol μm^{-2} s^{-1} and $V_{m,myo}$=1 mmol l^{-1} s^{-1} (A,B), during steady-state with a threefold increase in $V_{m,mito}$ and $V_{m,myo}$ (C,D), and during steady-state with a sevenfold increase in $V_{m,mito}$ and $V_{m,myo}$ (E,F).

experimental reductions in pH_i in invertebrate muscle lead to a reduction in AP concentration (Combs and Ellington, 1995). Considering that our exercise protocol leads to substantial lactate production in all size classes (Johnson et al., 2004), and since pH recovers with a time course similar to AP in blue crab dark muscle (Milligan et al., 1989), it is possible that a reduced pH_i in the dark fibers induces a transient shift in the AK equilibrium constant and slows the rate of AP recovery in both small and large fibers. However, it is unlikely that cellular acidosis can explain the differences in the rate of AP recovery between the small and large fibers, since in adult animals the dark levator pH_i recovers to resting levels much faster than extracellular pH or lactate concentration, despite the fact that anaerobic metabolism continues after contraction (Milligan et al., 1989). However, the processing of accumulated lactate may contribute to the differences between size classes. There is evidence that gluconeogenesis occurs in swimming muscle of blue crabs, and since there is no known designated site for lactate processing in crustaceans comparable to the mammalian liver, there is no Cori cycle (Milligan et al., 1989; Lallier and Walsh, 1991; Henry et al., 1994). Thus, lactate diffusing into the dark fibers of adult crabs may be used as a substrate for gluconeogenesis. Since gluconeogenesis and glycolysis are reciprocally controlled, aerobic AP recovery may be slowed in the large fibers because they are supplied with lactate, whereas the small fibers are not.

An unexpected finding of Johnson et al. (Johnson et al., 2004) was that there was significant post-contractile lactate accumulation in the dark fibers of the adult crabs, since it was assumed that their subdivisions alleviate the need for anaerobic contributions during recovery. They reasoned that this accumulation was likely a consequence of the dark fiber's close proximity to lactate-producing light fibers and net diffusive flux into the dark fibers from the lactate-laden hemolymph, and not a result of post-contractile anaerobic glycogenolysis occurring within the dark fibers. This supposition is supported by our

observation that large dark fibers have no significant post-contractile glycogen depletion (Fig. 4). This is in contrast to large light fibers, which produce copious lactate and significantly deplete glycogen post-contraction (Boyle et al., 2003; Johnson et al., 2004).

Though the large fibers did not exhibit any significant post-contractile glycogen depletion, we did observe a sharp, yet non-significant decrease in glycogen immediately after exercise. This depletion may result from anaerobic glycogenolysis, which increasingly powers burst contractions in these fibers as AP is depleted, although a similar contraction-induced decrease was not observed in small fibers despite producing an identical amount of lactate. This same pattern of post-contractile glycogen depletion was observed by Henry et al. (Henry et al., 1994) in adult blue crab dark fibers following vigorous exercise, indicating that this may be a typical response to burst contractile activity. Although we did not observe any significant post-contractile glycogen depletion in the large fibers as expected, we did see an unexpected depletion of glycogen during recovery in the small fibers. Boyle et al. (Boyle et al., 2003), who measured post-contractile glycogen dynamics in blue crab light fibers, reported no significant glycogen depletion during recovery in the juveniles. However, immediately after exercise and before sacrifice the animals in their study were fed, potentially restoring depleted glycogen pools during the several hours of recovery. In our study, animals were not provided with a food source during recovery. We speculate that with no glycogen storing organ (van Aardt, 1988; Lallier and Walsh, 1991; Henry et al., 1994), as in the mammalian liver, and with no new source of glucose from a food supply, glycogen pools diminished by aerobic glycogenolysis during recovery could not be replenished to resting levels.

Kinsey et al. (Kinsey et al., 2005) used the same mathematical reaction–diffusion model used in the present study to investigate whether diffusion was limiting to AP recovery in the blue crab anaerobic light muscle; a fiber with extreme proportions, but a relatively low aerobic capacity (and hence low rate of ATP production). They found only small intracellular concentration gradients of high-energy phosphates during simulations of AP recovery. However, gradients became more substantial as the mitochondrial reaction rate was increased, which illustrated the interaction between diffusion limitation and ATP turnover rates. Intracellular diffusive flux does not appear to exert substantial control over AP recovery in the blue crab giant light fibers, but there may be other cell types where diffusion is limiting. These are likely to include systems with a relatively high rate of ATP production/consumption such as the blue crab dark fibers, which have a 10-fold higher mitochondrial density than the light fibers. However, our reaction–diffusion analysis revealed no intracellular concentration gradients of high-energy phosphates during a burst contraction–recovery cycle at the rates of AP recovery determined for the dark fibers (Fig. 5). This is not surprising considering that AP recovery rates in dark fibers were similar to those found previously for light fibers (Kinsey et al., 2005), although it is likely that a less intense exercise protocol may have allowed higher recovery rates in dark fibers by reducing lactate production (see above). In fact, in prior simulations where the mitochondrial rate was increased to yield AP recovery rates that were comparable to that observed in aerobic mammalian muscle, substantial gradients were observed (Kinsey et al., 2005). Nevertheless, even the fast rate of recovery that was observed in the dark fibers of the small animals was too slow to be limited by intracellular metabolite diffusion, which is consistent with the analysis of light fibers by Kinsey et al. (Kinsey et al., 2005).

Although post-contractile AP recovery in the dark fibers does not appear to be limited by diffusion, these aerobic fibers normally power steady-state contraction during sustained swimming. Under these conditions, ATP turnover rates are much higher than they are during post-contractile recovery. Using a myosin ATPase rate that was 25% of that used for burst contraction and a $V_{m,mito}$ that is comparable to that of prior studies (see Vicini and Kushmerick, 2000), we observed substantial concentration gradients in AP and ATP, as well as other metabolites, during simulated steady-state contraction. As expected, the gradients became more substantial as the ATP turnover rate was increased (Fig. 6). The ATP buffering role of AK is apparent since at relatively low rates of demand ATP gradients are minimal, but as AP is depleted ATP gradients become severe. Thus, it appears that AP recovery in blue crab dark fibers is not limited by diffusion at the low rates of ATP turnover that seem to characterize our burst contraction–recovery protocol, but despite the short intracellular diffusion distances resulting from fiber subdivisions, the high rates of ATP turnover observed during steady-state contraction result in substantial metabolite gradients.

In summary, the patterns of recovery that have been observed in blue crab locomotor muscles previously (Boyle et al., 2003; Johnson et al., 2004; Kinsey et al., 2005), and herein, suggest that there are effects of fiber size on aerobic metabolism. Although the aerobic dark fibers are as large as the anaerobic light fibers, the selective pressure to power aerobic swimming has promoted the evolution of an intricate network of mitochondria-rich, highly perfused subdivisions. These subdivisions allow the fibers to retain a small metabolic functional unit while apparently developing a large contractile functional unit during growth, thereby eliminating the need for anaerobic contributions to recovery in adult animals. Our reaction–diffusion analysis, in conjunction with observed AP recovery data, suggests that intracellular diffusion does not limit aerobic recovery in blue crab levator fibers, as expected. However, the rates of AP recovery in the dark fibers were considerably lower than expected, considering the high mitochondrial density of these fibers, and this was probably due to metabolic inhibition. During simulated steady-state contraction, intracellular metabolite diffusion did limit aerobic metabolism, suggesting that diffusion may exert substantial control over aerobic flux even in small fibers if the ATP turnover rate is high.

This research was supported by National Science Foundation grants to S.T.K. (IBN-0316909) and B.R.L. (IBN-0315883), as well as a Sigma Xi Grant-in-Aid of Research to K.M.H.

References

Beis, I. and Newsholme, E. A. (1975). The contents of adenine nucleotides, phosphagens and some glycolytic intermediates in resting muscles from vertebrates and invertebrates. *Biochem. J.* **152**, 23-32.

Bird, R. B., Stewart, W. E. and Lightfoot, E. N. (1960). *Transport Phenomena*. New York: Wiley.

Boyle, K. L., Dillaman, R. M. and Kinsey, S. T. (2003). Mitochondrial distribution and glycogen dynamics suggest diffusion constraints in muscle fibers of the blue crab, *Callinectes sapidus*. *J. Exp. Zoolog. Part A Comp. Exp. Biol.* **297**, 1-16.

Brody, S. (1945). *Bioenergetics and Growth*. New York: Reinhold.

Combs, C. A. and Ellington, W. R. (1995). Graded intracellular acidosis produces extensive and reversible reductions in the effective free energy change of ATP hydrolysis in a molluscan muscle. *J. Comp. Physiol. B* **165**, 203-212.

deFur, P. L., Pease, A., Siebelink, A. and Elfers, S. (1988). Respiratory responses of blue crabs, *Callinectes sapidus*, to emersion. *Comp. Biochem. Physiol.* **89A**, 97-101.

Hancock, C. R., Brault, J. J., Wiseman, R. W., Terjung, R. L. and Meyer, R. A. (2005). ^{31}P-NMR observation of free ADP during fatiguing, repetitive contractions of murine skeletal muscle lacking AK1. *Am. J. Physiol.* **288**, C1298-C1304.

Harris, R. C., Edwards, R. H. T., Hultman, E., Nordesjö, L. O., Nylind, B. and Sahlin, K. (1976). The time course of phosphorylcreatine resynthesis during recovery of the quadriceps muscle in man. *Pflugers Arch.* **367**, 137-142.

Henry, R. P., Booth, C. E., Lallier, F. H. and Walsh, P. J. (1994). Post-exercise lactate production and metabolism in three species of aquatic and terrestrial decapod crustaceans. *J. Exp. Biol.* **186**, 215-234.

Holt, S. M. and Kinsey, S. T. (2002). Osmotic effects on arginine kinase flux in muscle from the blue crab. *J. Exp. Biol.* **205**, 1775-1785.

Hubley, M. J., Locke, B. R. and Moerland, T. S. (1997). Reaction-diffusion analysis of effects of temperature on high-energy phosphate dynamics in goldfish skeletal muscle. *J. Exp. Biol.* **200**, 975-988.

Johnson, L. K., Dillaman, R. M., Gay, D. M., Blum, J. E. and Kinsey, S. T. (2004). Metabolic influences of fiber size in aerobic and anaerobic muscles of the blue crab, *Callinectes sapidus*. *J. Exp. Biol.* **207**, 4045-4056.

Keppler, D. and Decker, K. (1974). Glycogen determination with amyloglucosidase. In *Methods of Enzymatic Analysis.* Vol. 3 (ed. H. U. Bergmeyer), pp. 1127-1131. New York: Academic Press.

Kim, S. K., Yu, S. H., Jeong-Hwa, S., Hübner, H. and Buchholz, R. (1998). Calculations on O_2 transfer in capsules with animal cells for the determination of maximum capsule size without O_2 limitation. *Biotech. Lett.* **20**, 549-552.

Kinsey, S. T. and Moerland, T. S. (2002). Metabolite diffusion in giant muscle fibers of the spiny lobster, *Panulirus argus*. *J. Exp. Biol.* **205**, 3377-3386.

Kinsey, S. T., Penke, B., Locke, B. R. and Moerland, T. S. (1999). Diffusional anisotropy is induced by subcellular barriers in skeletal muscle. *NMR Biomed.* **11**, 1-7.

Kinsey, S. T., Pathi, P., Hardy, K. M., Jordan, A. and Locke, B. R. (2005). Does metabolite diffusion limit post-contractile recovery in burst locomotor muscle? *J. Exp. Biol.* **208**, 2641-2652.

Kushmerick, M. J., Meyer, R. A. and Brown, T. R. (1992). Regulation of oxygen consumption in fast- and slow-twitch muscle. *Am. J. Physiol.* **263**, C598-C606.

Lallier, F. H. and Walsh, P. J. (1991). Metabolic potential in tissues of the blue crab, *Callinectes sapidus*. *Bull. Mar. Sci.* **48**, 665-669.

Mainwood, G. W. and Raukusan, K. (1982). A model for intracellular energy transport. *Can. J. Physiol. Pharmacol.* **60**, 98-102.

McMahon, S. and Jenkins, D. (2002). Factors affecting the rate of phosphocreatine resynthesis following intense exercise. *Sports Med.* **32**, 761-784.

Meyer, R. A. (1988). A linear model of muscle respiration explains monoexponential phosphocreatine changes. *Am. J. Physiol*. **254**, C548-C553.

Meyer, R. A., Brown, T. R., Krilowicz, B. L. and Kushmerick, M. J. (1986). Phosphagen and intracellular pH changes during contraction of creatine-depleted rat muscle. *Am. J. Physiol.* **250**, C264-C274.

Milligan, C. L., Walsh, P. J., Booth, C. E. and McDonald, D. L. (1989). Intracellular acid-base regulation during recovery from locomotor activity in the blue crab, *Callinectes sapidus*. *Physiol. Zool.* **62**, 621-638.

Roer, R. and Dillaman, R. (1984). The structure and calcification of the crustacean cuticle. *Am. Zool.* **24**, 893-909.

Sahlin, K., Harris, R. C. and Hultman, E. (1975). Creatine kinase equilibrium and lactate content compared with muscle pH in tissue samples obtained after isometric exercise. *Biochem. J.* **152**, 173-180.

Schmidt-Nielsen, K. (1984). *Scaling: Why is Animal Size so Important?* New York: Cambridge University Press.

Smith, E. and Morrison, J. F. (1969). Kinetic studies on the arginine kinase reaction. *J. Biol. Chem.* **244**, 4224-4234.

Teague, W. E. and Dobson, G. P. (1999). Thermodynamics of the arginine kinase reaction. *J. Biol. Chem.* **274**, 22459-22463.

Tse, F. W., Govind, C. K. and Atwood, H. L. (1983). Diverse fiber composition of swimming muscles in the blue crab, *Callinectes sapidus*. *Can. J. Zool.* **61**, 52-59.

van Aardt, W. J. (1988). Lactate metabolism and glucose patterns in the river crab, *Potamonautes warreni* Calman, during anoxia and subsequent recovery. *Comp. Biochem. Physiol.* **91A**, 299-304.

van den Thillart, G. and Waarde, A. V. (1993). The role of metabolic acidosis in the buffering of ATP by phosphagen stores in fish: an in vivo NMR study. In *Surviving Hypoxia: Mechanisms of Control and Adaptation* (ed. P. W. Hochachka, P. L. Lutz, T. Sick, M. Rosenthal and G. van den Thillart), pp. 237-252. Orlando: CRC.

Vicini, P. and Kushmerick, M. (2000). Cellular energetics analysis by a mathematical model of energy balance: estimation of parameters in human skeletal muscle. *Am. J. Physiol. Cell Physiol.* **279**, C213-C224.

White, C. R. and Seymour, R. S. (2003). Mammalian basal metabolic rate is proportional to body mass. *Proc. Natl. Acad. Sci. USA* **100**, 4046-4049.